Chapter 5

# Metallic and Oxide Electrodeposition

Eric M. Garcia, Vanessa F.C. Lins and Tulio Matencio

Additional information is available at the end of the chapter

http://dx.doi.org/10.5772/55684

## 1. Introduction

Electrodeposition of metals or its oxides is one of oldest themes in electrochemical science [1-6]. The first studies on this topic are dated from early nineteenth century, using galvanic cells as a power source [3-6]. Despite the antiquity, electrodeposition remains a much studied topic. Themes as supercapacitors or electrochemical cells devices have raised considerable attention [7-17]. In this case, the electrodeposition technique is of great interest due to their unique principles and flexibility in the control of the structure and morphology of the oxide electrodes.

One of the most modern applications of oxides electrodeposition is solar cells. Investigation of the development of environmentally friendly low cost solar cells with cheaper semiconductor materials is extremely important for the development of green energy technology. The electrodeposition of $Cu_2O$, $TiO_2$ and many others oxides, is a very promissory research field due the low cost and high efficiency of this electrochemical method.

Moreover, two new topics that also deserves attention is the application of electrodeposition in solid oxide fuel cells (SOFC) and the metals recycling. In this field of study the electrodeposition also contributes very significantly. For SOFC, the electrodeposition is used to formation of protective coating on electrical interconnects. By other hand, in the metal recycling, the electrodeposition is the cheaper and simple method by obtention of metallic elements.

Thus, in this chapter will be reported some theoretical aspects about electrodeposition of metals and oxides and their applications more modern and relevant. Among these applications will be treated with one application of electrodeposition in supercapacitors, solar cells, recycling of metals and electrical interconects for solid oxide fuel cells (SOFC).

### 1.1. Theoretical foundation of electrodeposition

In the early stages of electrodeposition, the limiting step corresponds to electrons transfer from work electrode for metallic ions in solution. In this case the relation between the current and the overpotential for electrodeposition is given by Eq. 1 [1-4]. In this equation, F is Faraday's constant, k is a constant, C is the concentration of metal ions in solution, $\alpha$ corresponds to a coefficient of symmetry (near 0.5), $\eta$ corresponds to overpotential, R is the ideal gas constant and T the absolute temperature, in Kelvin. There is an exponential dependence between the current and applied overpotential. Obviously that, with increasing of overpotential, the ionic current that electrolyte can supply is limited by the other processes as such material transport or electrical conductivity [2]. Through Coulomb's law, we obtain the relation of thickness with the charge density ($d = MMq/nF\varrho$). Where, MM corresponds to the molecular weight, q is the charge density, n corresponds the charge of metal ions and $\varrho$ is the density.

$$i = -FkC\exp\left(\frac{\alpha F\eta}{RT}\right) \tag{1}$$

In electrodeposition, is very common the use of potential versus current curves called voltammetry. The figure 1-a shows a typical cyclic voltammetry for cobalt electrodeposition on a steel electrode. The cyclic voltammetry is used to identify the potential where begins the electrodeposition and the electrodissolution. In cathodic scan, for potential more negative than -0.70 V occurs the $Co^{+2}$ reductions for metallic cobalt onto steel electrode. In anodic scan, the cobalt dissolution begins in -0.3 V. The voltammogram shown in figure 1-a represents the cobalt electrodeposition, however, many others metallic electrodeposition follow the same pattern.

In the electrodeposition of $M^{n+}$ ions using the aqueous media (Eq. 2) is always observed the hydrogen evolution reaction (HDR) represented by equation 2. This results principally in reducing the loading efficiency of electrodeposition [1-5].

$$M^{n+}_{(aq)} + ne^- \rightarrow M_{(s)} \tag{2}$$

$$2H^+_{(aq)} + 2e^- \rightarrow H_{2(g)} \tag{3}$$

The charge efficiency is an important aspect in metal electrodeposition. In this case, the parallel reaction showed in the equations 2 has a great influence in the electrodeposition. The figure 1b shows the charge efficiency for cobalt electrodeposition in pH = 1.50 (high concentration of $H^+$) and pH = 6.00 (low concentration of $H^+$). In pH = 1.50 note that the maximum efficiency (about 68%), while in pH = 6.00 the charge efficiency value can easily reach 95%. This occurs because at high concentrations of $H^+$, part of charge is used for promotes the reaction shown

http://dx.doi.org/10.5772/55684

by Equation 2. In pH =6.00 the concentration of $H^+$ is very low compared with cobalt concentration, thus, the cobalt electrodeposition is the principal reaction.

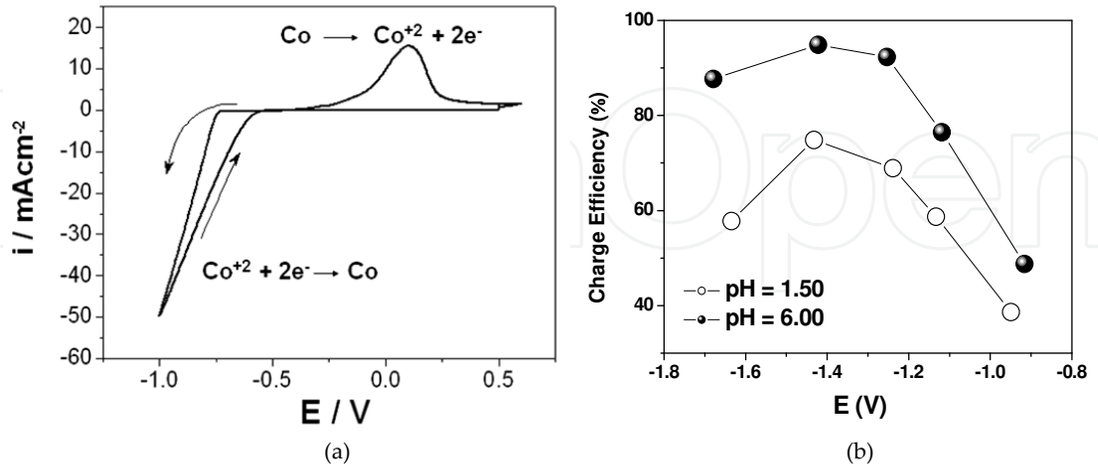


**Figure 1.** a) Cobalt electrodeposition on a platinum electrode. The ionic concentration of $Co^{+2}$ is 1.00 $molL^{-1}$ and the scan rate was 1 $0mVs^{-1}$. (b) Charge efficiency for cobalt electrodeposition in a range of potentials, and at pH 1.50 and 6.00.

The morphological aspects are also influenced by parallels reactions[1,2,3].The figure 2 shows the metallic cobalt electrodeposited on ferritic steel in pH = 1.50 and 6.00. It clearly appears that the deposit at pH = 1.50 is more compact than the deposit at pH = 6.00. According to many authors this effect appears due the $H^+$ reduction onto surface of growth islands. The application of the nucleation models to the initial electrodeposition stages shows that at pH=6.00, the nuclei grow progressively (progressive nucleation). SEM showed a three-dimensional nucleus growth. With the decrease in pH to 1.50, the nucleation process becomes instantaneous (instantaneous nucleation).

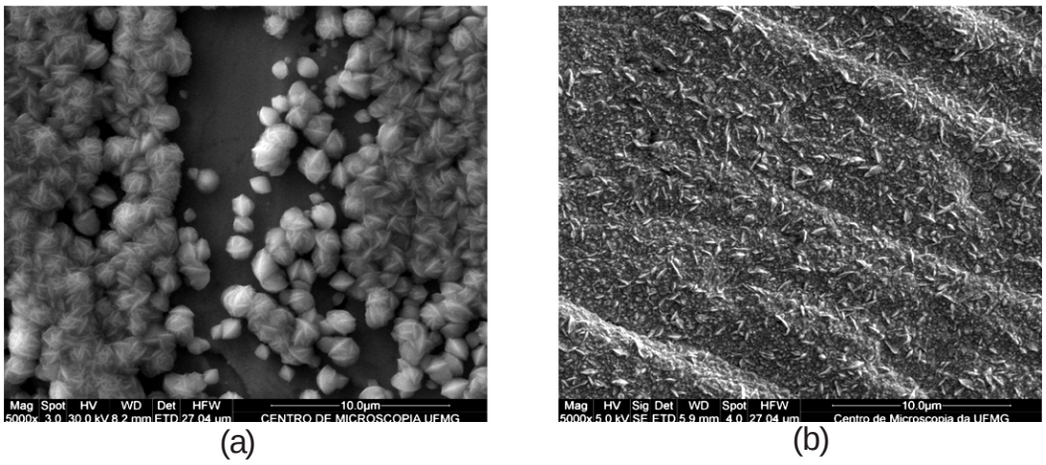


**Figure 2.** Scanning Electron Microscopy images of cobalt electrodeposited in: (a) pH= 6.00 and (b) pH 1.50. The potential applied of –1.00 V and charge density was 10.0 C $cm^{-2}$ and the electrolyte was $CoSO_4$ 1 $molL^{-1}$.

### 1.2. Oxide electrodeposition

In the electrodeposition of oxides, more of a method can be adopted. From a metal layer previously electrodeposited can be performed a polarization in alkaline solution such as NaOH, KOH etc. This results can be expressed by equations 4 and 5. The first step is the metal dissolution that is an electrochemical process (Eq. 4). The second step (Eq. 5) is the chemical process due precipitation of hydroxide on the surface of substrate. This method produces films with high adherence and a reduced thickness. This probably occurs due to formation of an oxide layer on a metal layer with a high surface area [4-5].

$$M_{(s)} \rightarrow M_{(aq)}^{n+} + ne^{-} \tag{4}$$

$$M_{(aq)}^{n+} + OH_{(aq)}^{-} \rightarrow M(OH)_{n(ads)} \tag{5}$$

Figure 3-a shows an electrodeposited layer of cobalt over a stainless steel. Figure 3-b represents the cobalt film after a potentiostatic polarization at 0.7 V (Ag / AgCl reference) during 200 s. The electrolyte used was NaOH 6 molL$^{-1}$.

The cobalt film electrodeposited showed a high contact area. This can also be visualized in the oxide/ hydroxide formed after the anodic polarization in NaOH 6 molL$^{-1}$.

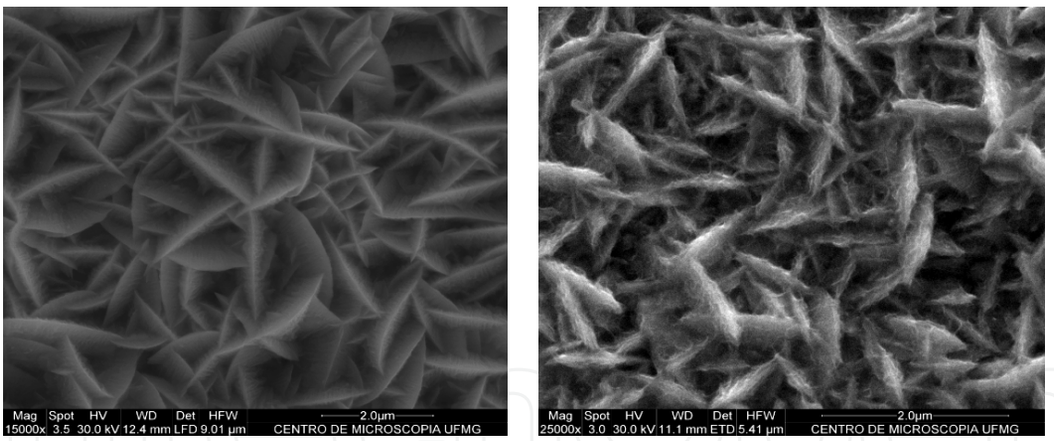


**Figure 3.** *Scanning electron microscopy images of (a) Cobalt electrodeposition on a steel electrode.(b)* Cobalt film after a potentiostatic polarization at 0.7 V (Ag / AgCl reference) during 200 s in NaOH 6 molL$^{-1}$.

Another method frequently used for electrodeposition of hydroxides on the conductive substrates is the use of nitrates as counter ions. In this case the hydroxyl ions are generated by reduction of nitrate ions in solution (Eq. 5).. The film of metallic hydroxide is then generated as shown by Eq 4.

$$NO_{3(aq)}^{-} + 7H_2O + 8e^{-} \rightarrow NH_{4(aq)}^{+} + 10OH_{(aq)}^{-} \tag{6}$$

http://dx.doi.org/10.5772/55684

Another method used for the formation of metal oxides is the anodic electrodeposition In this case the equation that represents this generic reaction is shows in Eq 6.

$$M_{(aq)}^{n+} + mH_2O \underset{\leftarrow}{\rightarrow} Mn_2O_{n(s)} + 2mH_{(aq)}^{+} + ne^{-} \tag{7}$$

### 1.3. Electrodeposition morphology

Basically in the most papers, the electrodeposition can occur by passing a current fixed or by imposing a fixed potential. In both cases, the energy for the formation of nuclei for growth is given by Eq. 7 (the nucleation energy). In this equation, N* is the number of atoms per nucleus growth (cluster), $z_i$ is the charge of the metal ion, $e_0$ is the elementary charge and $|\eta|$ corresponds to the overpotential applied. The second term represents the increased surface tension caused by the addition of ad-atoms. Thus, the greater number of atoms larger the cluster size as shows in the Eq. 7. Optimizing the nucleation energy appropriately ($d\Delta G/d\eta=0$) we get the expression for maximum atoms number that each nuclei may contain (Eq. 8). where $\varepsilon$ is the surface energy and s is the area of each atom.

$$\Delta G = -N^{*} z_i e_0 |\eta| + \varphi(N) \tag{8}$$

$$N_{crit} = \frac{\pi \varepsilon^2 s}{(z_i e_0 \eta)^2} \tag{9}$$

Thus, it is not difficult to observe that the higher overpotential, lower the number of atoms per growth nucleus and consequently the smaller grain size obtained. The electrodeposition created under low overpotential have smaller grains, while samples prepared under high overpotential are formed by pyramidal structures. In fact this observation can also be seen in Figure 2. This Figure shows the SEM of electrodeposited cobalt obtained in 100 and 200 $mAcm^{-2}$. In the higher current density, the grain size is much smaller.

Now we can see that, unlike other deposition techniques, in the electrodeposition, the characteristics of formed film are related with simple parameters as pH and overpotential applied. This makes with this method became versatile and inexpensive compared to other deposition methods.

## 2. Modern applications of metallic electrodeposition

With the electrodeposition is possible to achieve very thin layers of metal over the other metal or another electrical conductor material. Since that a metallic film is onto conductive substrate is possible formation of oxide layers through electrochemical methods.

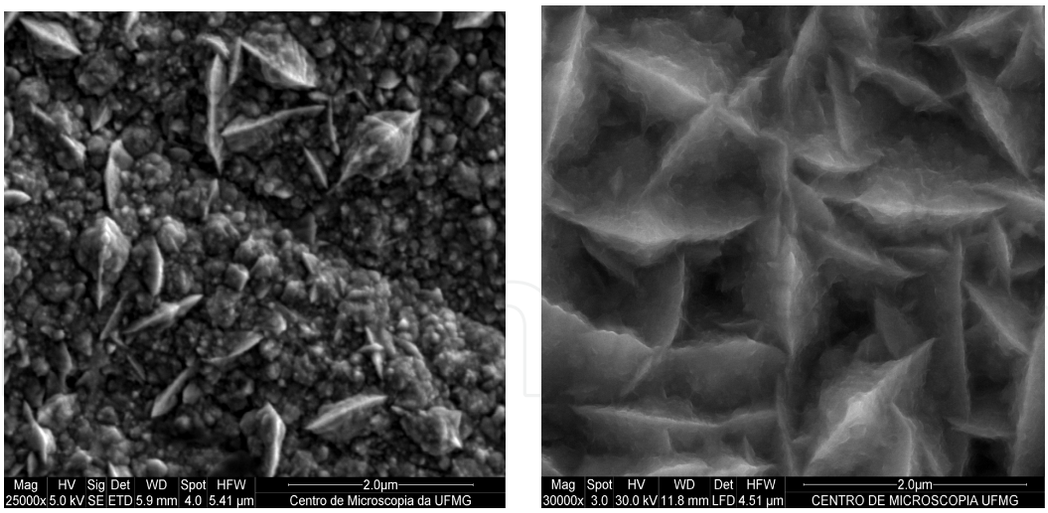


**Figure 4.** SEM images of cobalt electrodeposited from 0.5 molL$^{-1}$ sulphate cobalt at 200mAcm$^{-2}$ and (b) at 100 mAcm$^{-2}$.

### 2.1. Supercacitors

The energy always played an important role in human being's life [4]. Thus, it is necessary to study about renewable energy sources to reduce the energy consumption. Because this, the capacitors are used in the transport systems as a mean to store energy and reuse it during short periodic intervals. Basically, the conventional capacitors consist of two conducting electrodes separated by an insulating dielectric material and The application of this electrical device is the storage of energy.

When a voltage is applied to a capacitor, opposite charges accumulate on the surfaces of each electrode. The differential capacitance is defined as C = dQ/dV where V is the difference of potential between the capacitor plates and Q is the accumulated charge in the active surface of capacitor material. The geometric relation of capacitance can be providing by equation 3 [6-7]. Where A and d are the geometric area and distance between capacitors plates respectively. The ε and $\varepsilon^o$ are the dielectric constant between the plates (no unit) and the vacuum permittivity (8.8 x 10$^{-12}$ Fm$^{-1}$) respectively.

$$C = \frac{A\varepsilon\varepsilon^0}{d} \tag{10}$$

In this form C is given in Faraday (F). Thus, for practical applications the capacitors plates must have high area and very small separation distance. The first capacitors of carbon materials can provide the specific capacitances of 15 – 50 μFcm$^{-2}$ [8]. The materials with capacitance densities of one, two or more hundreds of Fcm$^{-2}$ or Fg$^{-1}$ have been denominated as"supercapacitors" or "ultracapacitors"[4-8]. There are two principal types of supercapacitors: (a) the double-layer capacitor, and (b) the redox pseudocapacitor, the latter being developed in this paper. The high performances of capacitors that work with reversible

redox reaction are known as supercapacitors. The most used and commercial supercapacitors are basically made of an oxide semiconductor with a reversible redox couple. This oxide has to show a transition metal ion, which must be able to assume different valences and strong bonding power.

Among the oxide materials for application in supercapacitors, ruthenium and iridium oxides have achieved more attention. In many cases the capacitance depends on the preparation method and the deposition of oxides materials. Capacitances up to 500 F/g [5] or 720 F/g are reported for amorphous water-containing ruthenium oxides [6-9]. The great disadvantages of $RuO_2$ is the high cost and its low porosity structure [9-10]. Thus in recent works great efforts were undertaken in order to find new and cheaper materials [4-6]. A cheaper and widely used alternative is the activated carbon. The specific capacitance of this material is about 800 F/g [6]. In this context the researchers have tried to develop a material having a low cost, high surface area, high conductivity and high stability in alkaline medium.

*2.1.1. Cobalt oxides*

Cobalt oxides are attractive in view of their layered structure and their reversible electrochemical reactions. The possibility of enhanced performance through different preparative methods, also interests the scientists. The spinel cobalt oxide $Co_3O_4$, for example, can be obtained from hydroxide cobalt (II) previously deposited onto a conductive substrate (steel for example). Is enough a thermal oxidation in 400 degrees in air atmosphere, for formation of $Co_3O_4$. In the $Co_3O_4$ oxide, the reversibility of both redox process ($Co^{+2}/Co^{+3}$) (Eq. 4) and (Eq. 5) ($Co^{+3}/Co^{+4}$) in KOH 6 $molL^{-1}$ is very high and promising for capacitive applications in electrochemical devices [7-14].

$$Co^{+2}_{(net)} + OH^{-}_{(aq)} \underset{\leftarrow}{\overset{\rightarrow}{}} [Co - OH_{(ads)}]^{+3} + e^{-} \tag{11}$$

$$[Co - OH_{(ads)}]^{+3}_{(ads)} + OH^{-}_{(aq)} \underset{\leftarrow}{\overset{\rightarrow}{}} [Co - O_{(ads)}]^{+4} + H_2O + e^{-} \tag{12}$$

In figure 3 is shown a schematic of obtaining $Co_3O_4$. The previously electrodeposited cobalt can be subjected to a anodic polarization in solution of KOH 6$molL^{-1}$. With a thermal treatment of 20 hours at a temperature of 400 $^{o}$C the phase $Co_3O_4$ is formed onto substrate. This procedure leads to the formation of a layer of chemical composition of $Co(OH)_2$ [8-9]. The Figure 5 represents a cyclic voltammetry of a steel electrode coated with metallic cobalt in KOH 6$molL^{-1}$. Note that the first peak (around -0.6 V) is related with the electrodissolution of cobalt (Eq. 13) that leads to the formation of $Co(OH)_2$ (Eq. 14) [11-12].

$$Co_{(s)} \rightarrow Co^{2+}_{(aq)} + 2e^{-} \tag{13}$$

$$Co^{2+}_{(aq)} + OH^{-}_{(aq)} \rightarrow Co(OH)_{2(ads)} \quad (14)$$

The second peak, around 0.0 V, is related to the formation of $Co(OH)_3$ (Eq.15) [6-10]. The scheme showed in figure 5-b shows the obtention of $Co_3O_4$ from thermal oxidation.

$$Co(OH)_{2(ads)} + OH^{-}_{(aq)} \rightarrow Co(OH)_{3(ads)} + 1e^{-} \quad (15)$$

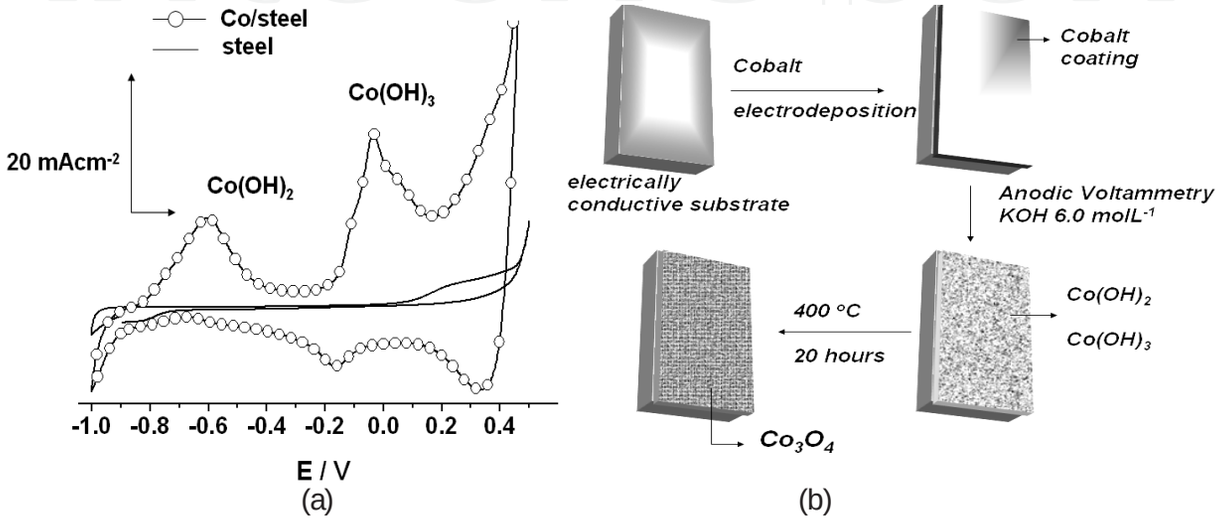


**Figure 5.** a) A cyclic voltammetry of a steel electrode coated with metallic cobalt in KOH 6molL$^{-1}$. (b) The obtention of $Co_3O_4$ from thermal oxidation.

There is also a method for the electrodeposition of a layer of $Co(OH)_2$ without the need for an alkaline solution. The $Co(OH)_2$ can be electrodeposited from a solution of cobalt nitrate. The many papers described this electrodeposition. The first step is the reduction of nitrate ions (Eq. 5). The reaction shown in the equation 5 promotes the alkalinization of electrical interface of metal "M". In a chemical step the Co(OH) is formed onto "M"(Eq. 6) [13-14].

$$NO^{-}_{3(aq)} + H_2O + 2e^{-} \rightarrow NO_{2(g)} + 2OH^{-}_{(aq)} \quad (16)$$

$$Co^{+2}_{(aq)} + 2OH^{-}_{(aq)} \xrightarrow{M} M / Co(OH)_{(s)} \quad (17)$$

In the vast majority of papers about supercapacitors based on cobalt oxides at least one of the steps corresponds to electrodeposition. In an interesting case in the literature, Kung et al [13] performed the electrodeposition of $Co(OH)_2$ on a Ti plate as shown by Eq.6. To obtain the $Co_3O_4$, the film of $Co(OH)_2$ it was submitted to an atmosphere ozone. They obtained an excellent capacitance specific value around 1000Fg$^{-1}$. Practically the same method however

with another the substrate, Zhou et al [14] obtained a specific capacitance of 2700Fg$^{-1}$. In this case the substrate was Ni. Are shown in table 1 some values of specific capacitance for oxides and hydroxides of cobalt found most frequently in literature.

| Method for $Co(OH)_2$ | Substrate | Specific capacitance | Solution | Method for $Co_3O_4$ | Reference |
|---|---|---|---|---|---|
| Potentiostatic | Ti plates | 1000 F g$^{-1}$ | $Co(NO_3)_2$ | Ozone | [13] |
| Potentiostatic | Ni sheets | 2700 F g$^{-1}$ | $Co(NO_3)_2$ | - | [14] |
| Cyclic voltammetry | Co electrodeposit | 310 Fg$^{-1}$ | LiOH | 150 °C | [15] |

**Table 1.** Some values of specific capacitance for oxides and hydroxides of cobalt obtained by electrodeposition or electrodeposition/calcination.

*2.1.2. Manganese oxides*

One promising material is hydrated amorphous or nanocrystalline manganese oxide, $MnO_2$ $nH_2O$ this material has exhibited capacitances exceeding 200 F/g in solutions of several alkali salts, such as LiCl, NaCl, and KCl [16]. Chang and Tsai [17] have reported supercapacitance of 240 Fg$^{-1}$ for hydrous $MnO_2$ synthesized by potentiostatic method. By other hand Feng et al [16] reported supercapacitors of 521 Fg$^{-1}$ for $MnO_2$ multilayer nanosheets prepared galvanostatically. Both in galvanostatic or potentiostatic electrodeposition, the anodic electrodeposition for formation of $MnO_2$ can be express by Eq. 7:

$$Mn^{+2}_{(aq)} + 2H_2O \underset{\leftarrow}{\overset{\rightarrow}{}} MnO_{2(s)} + 4H^{+}_{(aq)} + 2e^{-} \tag{18}$$

The model more relevant proposed to describe the charge and discharge cycles of $MnO_2$ at electrolyte constituted by $Na_2SO_4$ is given in Eq. 8. This equation demonstrated that the capacitance of MnO2 is result of redox reaction that occurs in its surface. This redox reaction corresponds of electrochemical adsorption/desorption of $Na^+$ ions [16-17].

$$MnO_{2(s)} + Na^{+}_{(aq)} + e^{-} \underset{\leftarrow}{\overset{\rightarrow}{}} (MnO_2{}^{-}Na^{+})_{ads} \tag{19}$$

A fact which makes the $MnO_2$ becomes most promising as supercapacitor, is the recycling Zn-$MnO_2$ batteries. Few studies in the literature report the recycling of Zn-$MnO_2$ batteries [18]. Thus, this line of research becomes extremely important to make supercapacitors based in $MnO_2$ more environmentally correct.

### 2.3. Solar cells

Photovoltaic (PV) cells are made up of two semi-conductor layers and one electrolyte. One layer containing a positive charge, the other a negative charge [19-22]. The n-type semiconductor receive radiation *hν*, thus valence electron is promoted to conduction band. One potential difference is established between the n-type semiconductor and the p-type semiconductor. This causes a photocurrent to flow through of the system. Basically, the electrolyte is used for circulation of ionic current which restores the nature of semiconductors. The figure 6 shows the scheme of photovoltaic cell. The researches are basically focuses on development of semiconductor electrodes and electrolytes cheaper and more efficient. Thus in this context the electrodeposition can contribute greatly. This is because the electrodeposition is a method simple, practical and inexpensive to produce both p-type as n-type [21,22].

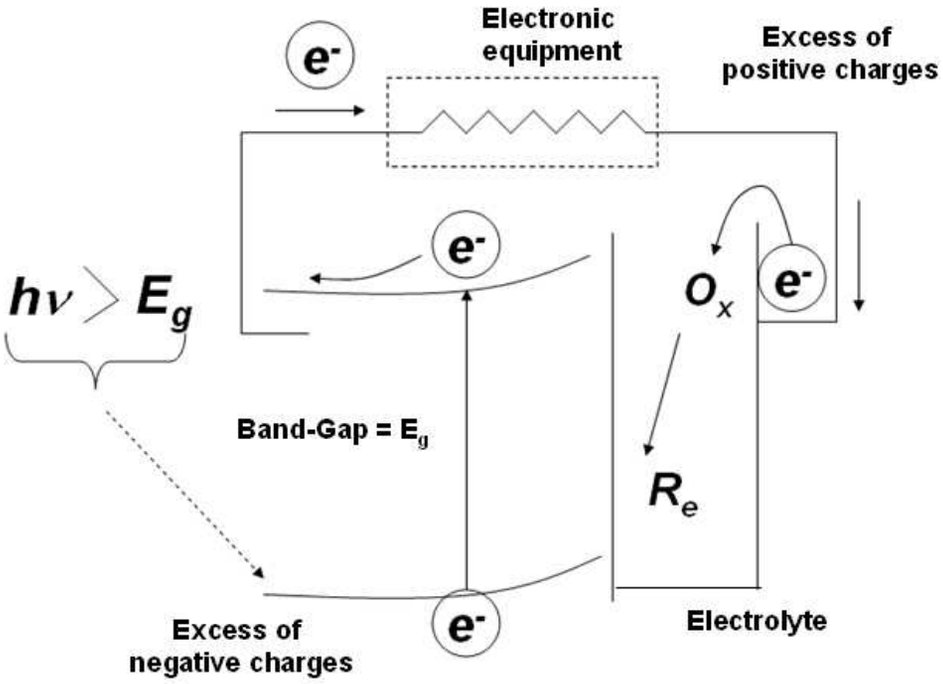


**Figure 6.** Representation of a photovoltaic cell using two semiconductor electrodes and an electrolyte.

#### *2.3.1. Semiconductive $Cu_2O$*

Among various transition metal oxides, cuprous oxide ($Cu_2O$) has attracted much attention. This because the $Cu_2O$ it is a non toxic and inexpensive semiconductor material. $Cu_2O$ is a direct band gap (1.80 eV) (Figure 7) semiconductor material and has a high absorption in the visible region of the solar spectrum [19,22,23].

The $Cu_2O$ may be a p-type semiconductor well as the n-type. In $Cu_2O$-p there are vacancies of cuprous ions ($Cu^+$) and in $Cu_2O$-n, there are oxygen vacancies. Many papers on the $Cu_2O$-p show that this material has a lower efficiency than 2% attributed to heterojunction represented by metallic cooper (Cu/$Cu_2O$-p) [22]. Thus, many studies have been focused on $Cu_2O$-n.

http://dx.doi.org/10.5772/55684

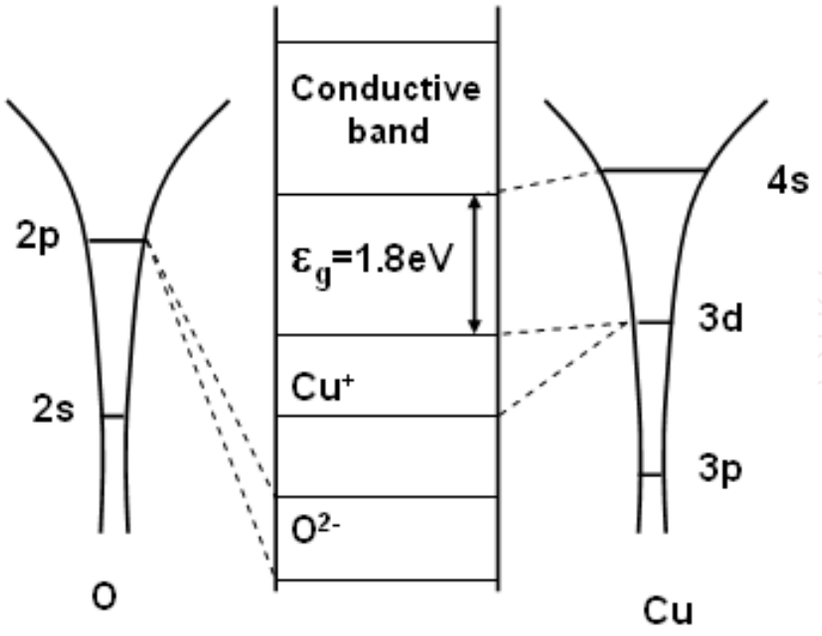


**Figure 7.** Representation of energy diagram for formation of $Cu_2O$.

Particularly, the obtention of *n*-type or *p*-type semiconductor can be controlled from pH of electrodeposition bath (Figure 8).

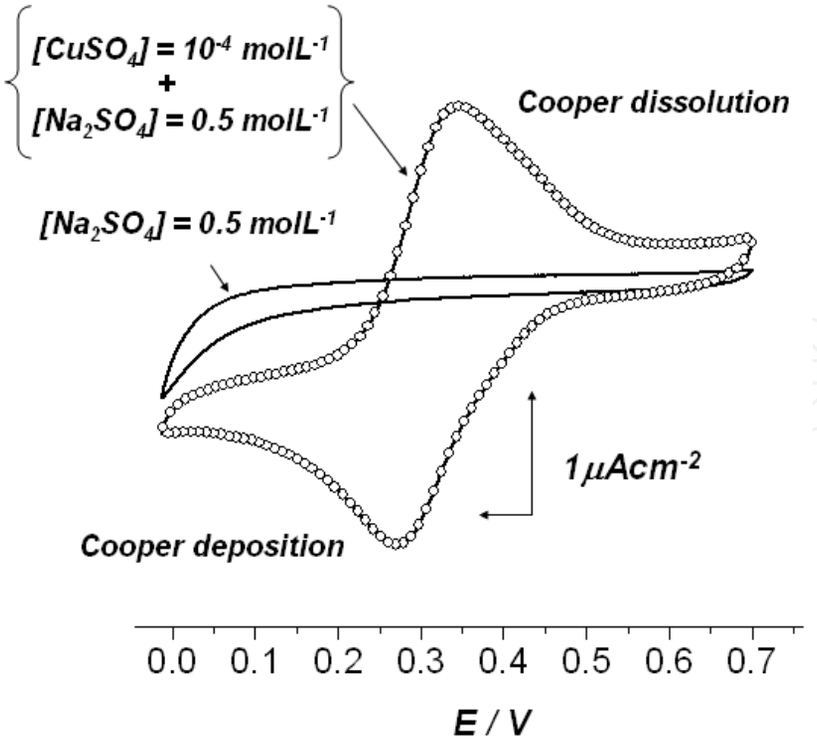


**Figure 8.** The cyclic voltammetry of a Pt electrode in $Na_2SO_4$ and $CuSO_4$ + $Na_2SO_4$ solution.

In copper electrodeposition several mechanisms are proposed. Considering the direct electrodeposition, the copper II ions are electrodeposited on one step as shown in Eq. 20. Siripala et al. [22] discusses the formation of an intermediate in the electrodeposition of copper. In this case the copper electrodeposition occurs through Cu+ forming the CuOH adsorbed (Eq. 21 and 22). Chemical occurs in one step the formation of $Cu_2O$ (Eq. 23).

$$Cu^{+2}_{(aq)} + 2e^- \rightarrow Cu_{(s)} \tag{20}$$

$$Cu^{+2}_{(aq)} + 1e^- \rightarrow Cu^{+}_{(aq)} \tag{21}$$

$$Cu^{+}_{(aq)} + OH^{-}_{(aq)} \rightarrow CuOH_{(ads)} \tag{22}$$

$$CuOH_{(ads)} + CuOH_{(ads)} \rightarrow Cu_2O + H_2O \tag{23}$$

The reason for formation of $Cu_2O$ is due to oxygen reduction forming peroxide. Among other electrochemical steps, one of the possible reactions in this case is shows in Eq. 24. The presence of $Cu^+$ certainly favor the formation of $Cu_2O$.

$$H_2O_{2(aq)} + Cu^{+2}_{(aq)} \rightarrow 2Cu^{+}_{(aq)} + 2H^{+}_{(aq)} + O_{2(g)} \tag{24}$$

According to Siripala et al. the type semiconductor (p or n) can be determined by ph of solution. If the copper electrodeposition occurs in pH below of 6.00 is formed preferably the $Cu_2O$-n. For pH above 6.00, electrodeposition of $Cu_2O$-p occurs preferably [22,23].

### *2.3.1. Semiconductive $TiO_2$*

Many papers have discussed the dye-sensitized solar cell (DSC) due its promising efficiency in very low cost [19-25]. In the literature is found cathodic electrodeposition of $TiO_2$ nanoparticles on the optically transparent fluorine doped tin oxide-coated (FTO) glass [25]. This type of the oxide electrodeposition is already prepared. The deposition is made due to current of electrophoresis. In electrodeposition in pH higher than the zero charge point (PCZ) the particles $TiO_2$ are negatively charged. Thus one cathodic electrodeposition is unfavorable due to electrostatic repulsion. In low pH there is a tendency for formation of bubbles of hydrogen gas due to reduction of H + ions. This causes a partial occupation of the electrode surface by decreasing the efficiency of the process. The electrodeposition of $TiO_2$ on the FTO is pictured in the figure 9.

http://dx.doi.org/10.5772/55684

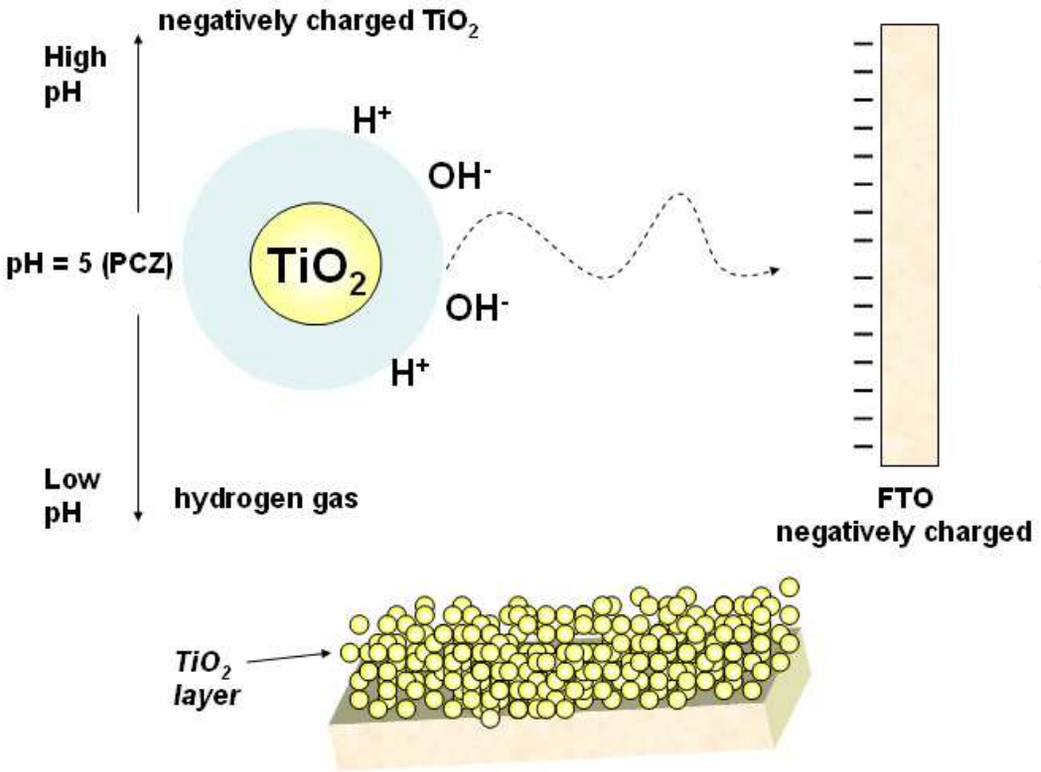


**Figure 9.** Representation of $TiO_2$ particles electrodeposition on F TO.

The-Vinh et al. [25] showed that the $TiO_2/SiO_2$ nanocomposite electrode facilitated the increase of ca. 20% of photocurrent density and ca. 30% of photovoltaic efficiency in comparison with the bare $TiO_2$ electrode. In accord to authors this electrodeposition method can be applied as an advanced microscopic way to control the electrochemical properties of the electrodes.

### 2.4. Electrical interconnects of Solid Oxide Fuel Cells (SOFCs)

In the current scenario where the researches are focused on cleaner energy sources and efficient, the fuel cells are gaining more space. Among the most promising fuel cells for generation of large quantity of power, are the solid oxide fuel cells (SOFCs) [26-29]. Solid oxide fuel cells (SOFCs) are solid-state devices that produce electricity by electrochemically combining fuel and air across an ionically conducting electrolyte. During operation of solid oxide fuel cell (SOFC) the anode is fed of hydrogen and cathode is supply with $O_2$ or air. At the operating temperature (600 to 800 °C), hydrogen is oxidized at the anode to $H^+$ ions. The freed electrons are conducted to the external circuit to the cathode, enabling the reduction of the oxygen ions $O^{-2}$(Eq.1.2) which are transported from the cathode to the anode through the electrolyte (ionic conductor). At the interface anode / electrolyte anions $O^{-2}$ react with $H^+$ to form $H_2O$ (1.3). Figure 10 depicts the scheme of operation of a SOFC.

In order to obtain high voltage and power density, a number of individual cells consisting of a porous anode, a dense thin-film electrolyte, and a porous cathode are electrically connected

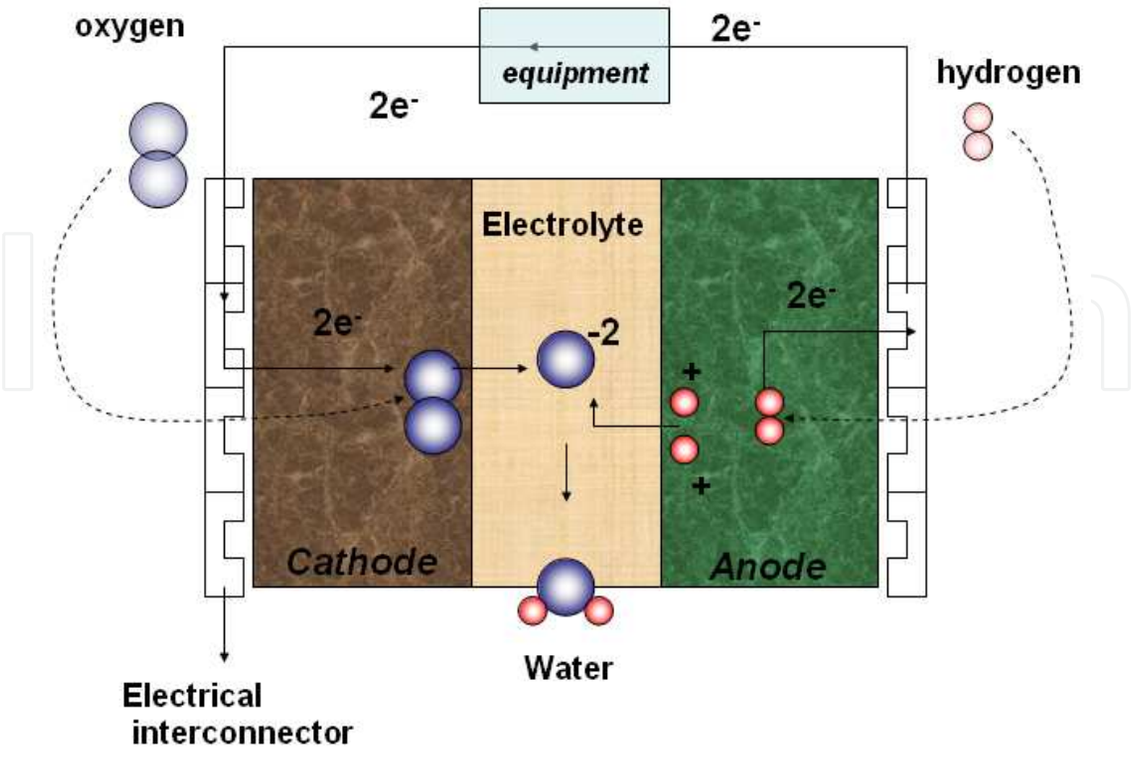


**Figure 10.** Simple scheme of operation and gases flow of a SOFC.

by interconnects to form a "stack". These interconnects are in contact with both electrodes (cathode and anode) and must meet a number of requirements [27-29] :

- Low area specific resistance (ASR). An acceptable value, after 40,000 working hours, is 0.10 Ohm $cm^{-2}$.
- Chemical stability in both atmospheres (reducing and oxidant) at high temperatures (between 600 and 1000 ºC).
- Impermeability to $O_2$ and $H_2$.
- Linear thermal expansion coefficient, LTEC, compatible with the other components of the cell (value close to 12.5 x $10^{-6}$ $K^{-1}$).

Metallic interconnects have attracted a great attention due to their high electronic and thermal conductivity and a low cost and good manufacturability compared to traditional ceramic interconnects [30]. In recent years, many works have been focused on ferritic stainless steel due to its low cost and adequate linear thermal expansion coefficient (11-12 x $10^{-6}$ $K^{-1}$) [28-30]. However, under the cathode working conditions (typically 800 ºC in air) $CrO_3$ evaporate from the $Cr_2O_3$ oxide film (Eq. 25) causing severe cell degradation [28-31].

$$\frac{1}{2}Cr_2O_{3(s)} + \frac{3}{4}O_{2(g)} \rightarrow CrO_{3(g)} \tag{25}$$

http://dx.doi.org/10.5772/55684

To improve the surface electrical properties and reduces the amount of chromium in the oxide film a coating of the stainless steel with semiconductor oxides has been proposed. Cobalt oxide $Co_3O_4$ is a promising candidate because of its interesting conductivity of 6.70 $Scm^{-1}$ and an adequate linear thermal expansion coefficient [32-33]. A good strategy to obtain the $Co_3O_4$ layer over stainless steel is cobalt electrodeposition with subsequent oxidation in air at high temperatures (SOFC cathode conditions) (Figure 11). The cobalt electrodeposition can be a low cost technique. This methodology initially a cobalt layer is electroplated on steel. Under the conditions cathode (air and ~ 800) occurs the formation of $Co_3O_4$. In the figure 12, is shown the MEV of a cobalt layer electrodeposited on a stainless steel plate.

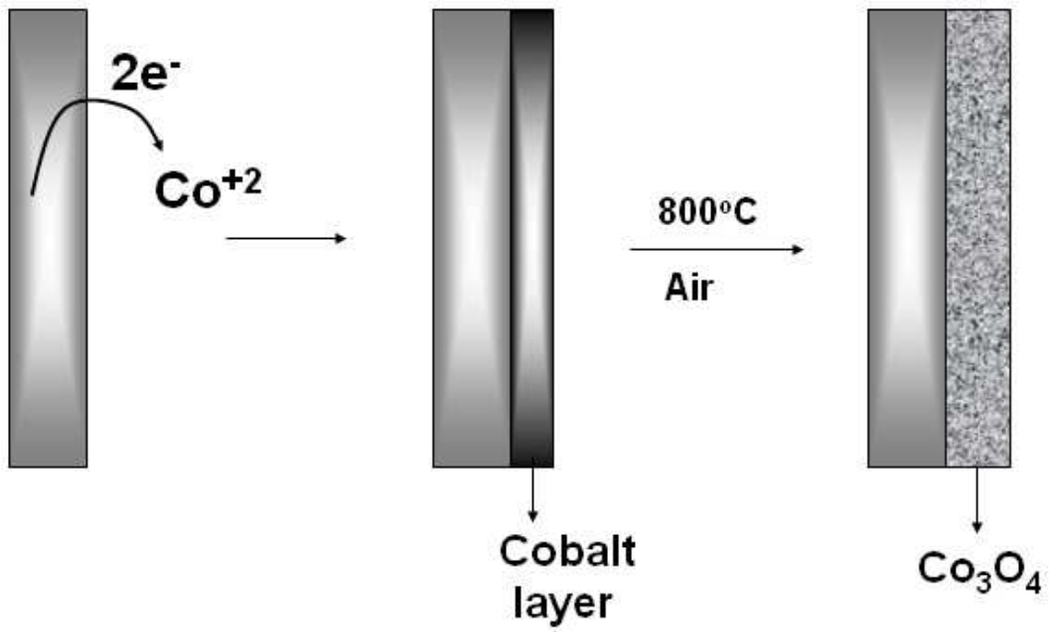


**Figure 11.** Scheme of $Co_3O_4$ obtention over stainless steel using the electrodeposition method.

The figure 13 shows that the steel without coating of cobalt subjected a strongly oxidizing conditions of cathode forms an oxide film very irregular. Also is observed that the steel surface shows the presence of chromium. Moreover the sample of coating steel with cobalt shows up very regular and without preença chromium in its surface.

In accord to Deng et al. [33] the stainless steel with electrodeposited cobalt tends to improve in high temperature and to reduce the chromium evaporation. The cobalt was oxidized to $Co_3O_4$. The coating not only maintains electrical contact, but it offers oxidation protection in ferritic stainless steels at lower chromium content and it is capable of significantly retarding chromium evaporation which reduces chromium poisoning of fuel cell. in accord to Wu et al [32], a uniform and smooth Mn–Co alloy can be successfully deposited on stainless steel substrate by electrodeposition. Compounds as $Mn_{1.5}Co_{1.5}O_4$ can reach an electrical conductivity of 90 $Scm^{-1}$ to 800 degrees [33]. This shows that the electrodeposition is an excellent alternative for achieving highly conductive films at high temperatures.

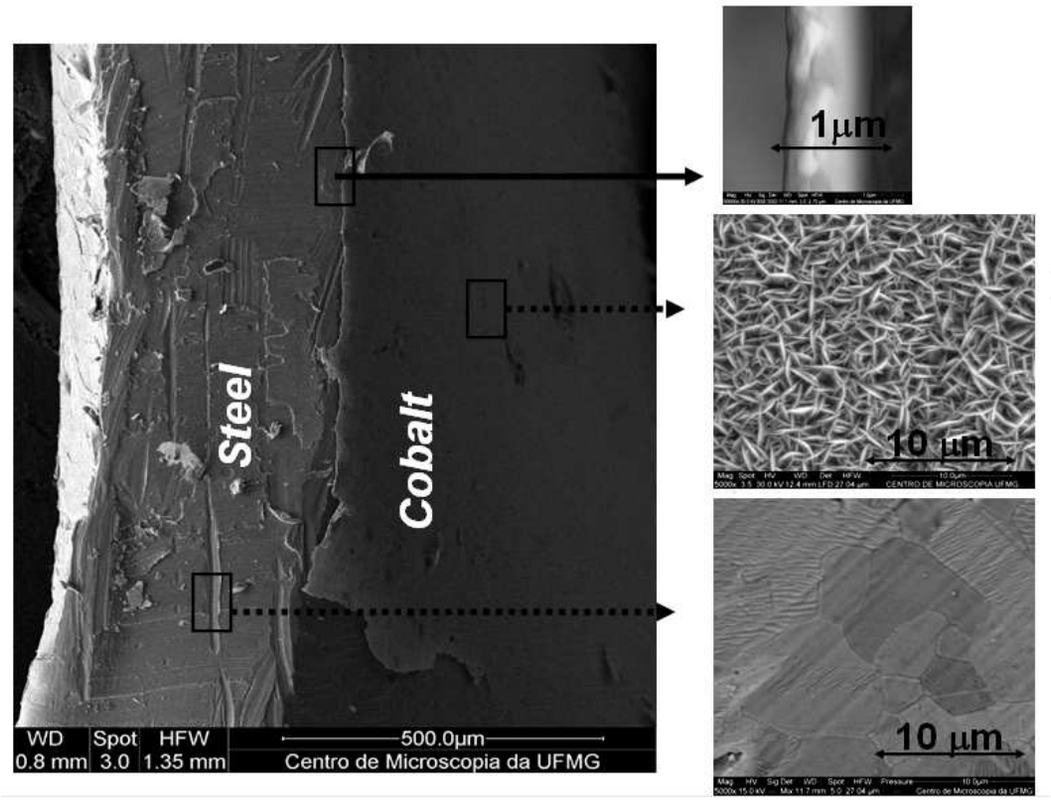


**Figure 12.** Scanning electron microscopy images of cobalt electrodeposited on stainless steel.

### 2.5. Ion-Li batteries recycling

The best way to achieve sustainable development is through recycling materials more precisely batteries. In this context, the electrodeposition takes shape more environmentally friendly. It is very interesting to note that metallic electrodeposition corresponds to a very interesting route for metal recycling. The principal metallic sources for recycling can be electronics circuits or spent batteries [6,34,35,36,37]. The Li-ion battery is a most attractive energy source for portable electronic products, such as cellular phones and laptop computers. Spinel structure $LiCoO_2$ is most used as the cathode material for Li-ion batteries due to its good performance in terms of high specific energy density and durability [1]. Thus, the Li-ion batteries are a valuable source of cobalt. The global reaction for charge and discharge of a li-ion battery with $LiCoO_2$ cathode can be represented b y Eq. 26. The $LiCoO_2$ is initially over the Al current collector. This is represented by figure 14.

$$LiCoO_2 + 6C \underset{\leftarrow}{\rightarrow} Li_{(1-x)}CoO + C_6Li_x \tag{26}$$

The first step in obtaining of cobalt from Li-ion batteries is removal of $LiCoO_2$ of current collector. This is accomplished by performing a heat treatment of cathode at 400 degrees for approximately 24 hours. The powder of $LiCoO_2$ obtained is dissolved in acidic solution under constant magnetic agitation at 80 ◦C for 2 h. The cathode dissolution efficiency increases with

http://dx.doi.org/10.5772/55684

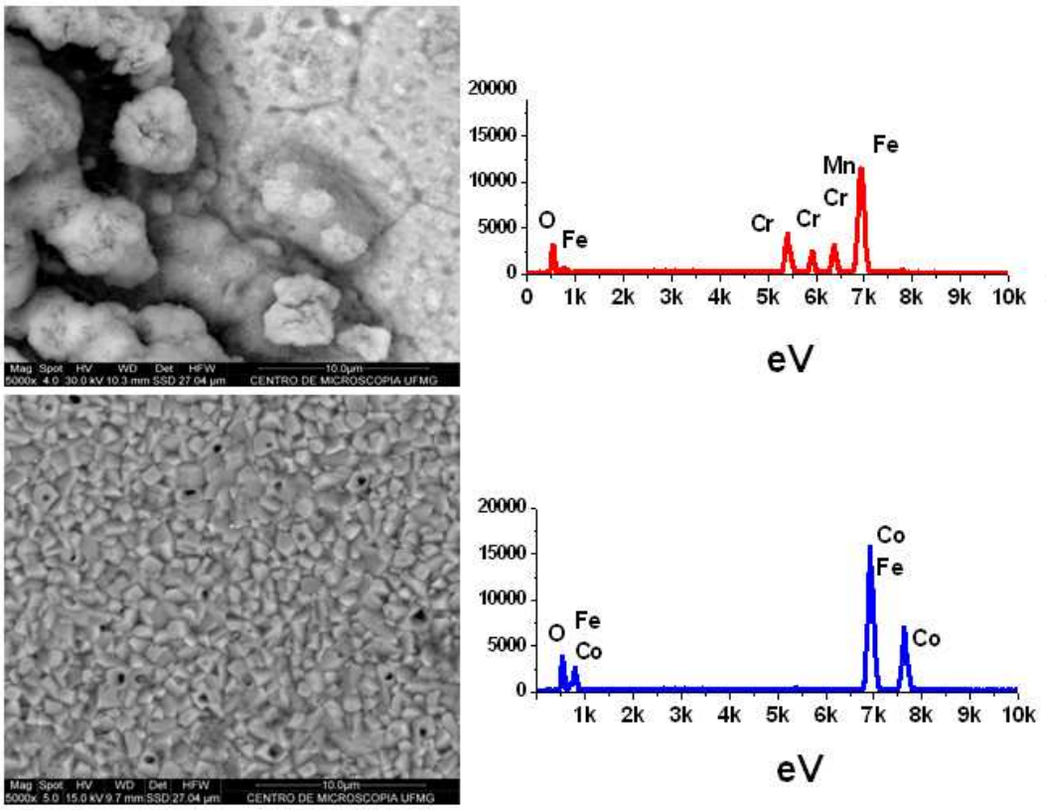


**Figure 13.** Scanning electron microscopy images and dispersive energy of X-ray for sample for steel coated with cobalt (low) and without cobalt (up) after 1000 hours at 850 degrees.

the increase of the acid concentration and temperature [6,34]. The addition of $H_2O_2$ is necessary to increase the efficiency of cathode dissolution. $H_2O_2$ reduces cobalt from oxidation state +III, insoluble in aqueous system, to +II, soluble in aqueous system. Considering that the active

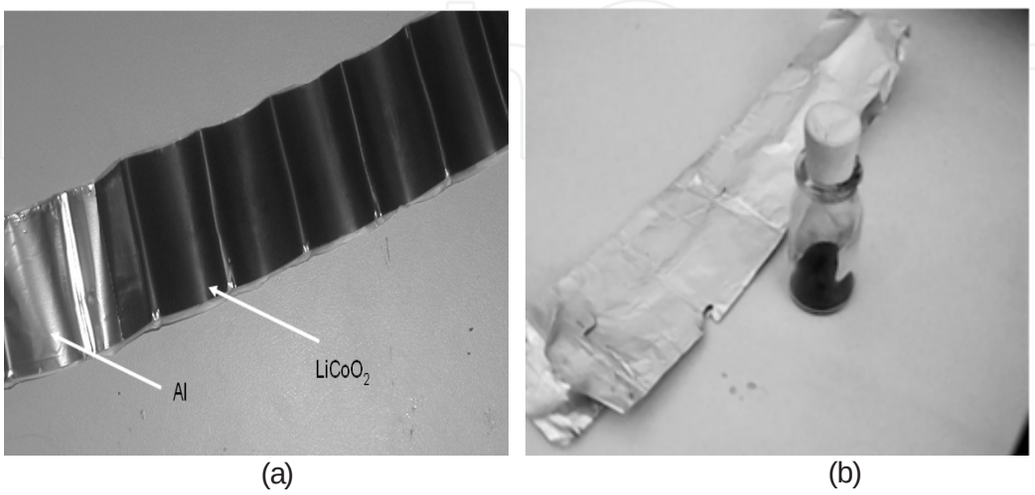


**Figure 14.** Photograph of the cathode of Li-ion batteries.

material is $LiCoO_2$, the cathode dissolution reaction is represented by Eq. (2) [6]. Figure 15 shows a simplified diagram of li-ion batteries recycling using the electrodeposition.

$$LiCoO_{2(s)} + \frac{1}{2}H_2O_{2(l)} + 3HCl_{(aq)} \rightarrow CoCl_{2(aq)} + \frac{1}{2}O_{2(g)} + LiCl_{(aq)} + 2H_2O_{(l)} \quad (27)$$

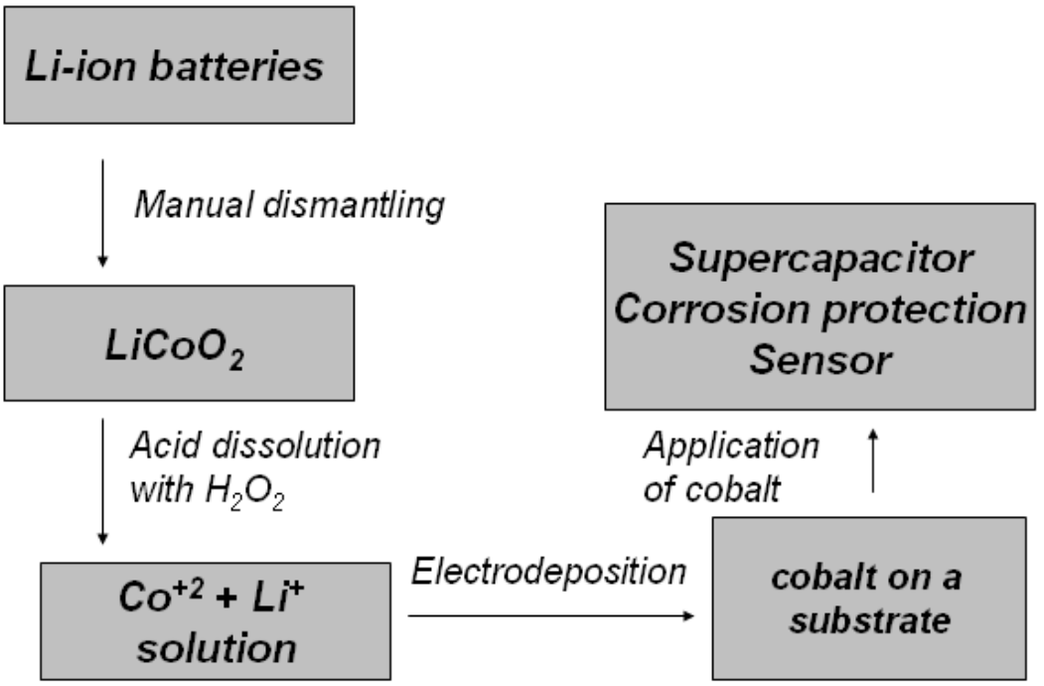


**Figure 15.** Simplified diagram of li-ion batteries recycling using the electrodeposition.

Although many groups working with Li-ion batteries recycling, the group most advanced in recycling via electrodeposition seems to be the group's researcher Eric M. Garcia. Garcia and other researchers perform a study of cathode Li-ion batteries recycling using the electrodeposition technique. Among several conclusions was shown that the largest charge efficiency found was 96.90% at pH 5.40. Furthermore, this research group conducted a detailed study of the mechanism of electrodeposition using electrochemistry quartz crystal microbalance technique (EQCM) [34]. In this case, it was assessed that at pH below 5, the electrodeposition of cobalt follows the direct mechanism (Eq. 13). For pH less than 2.70, cobalt electrodeposition occurs simultaneously with the reduction of protons to hydrogen [34]. In other work of Garcia and colleagues of research, it was explained the morphology of material electrodeposited with relation to pH. Although other research papers also focused on the cobalt electrodeposition as way of recycling battery Li-ion, Garcia's group pioneered the application of recycled cobalt. Garcia and other researchers associated the recycling of Li-ion battery to production of supercapacitor based on composite formed by cobalt oxides and hydroxides. The specific capacitances calculated from cyclic voltammetry and electrochemical impedance spectroscopy show a good agreement with the value of 625 $Fg^{-1}$ [36]. Moreover Garcia et al. also proposed

the application of recycled cobalt in interconnects for SOFC [37]. In this work the metallic cobalt was electrodeposited on 430 steel in order to obtain a low electrical resistance film made to $Co_3O_4$. After oxidation at 850 $^oC$ for 1000 h in air, the cobalt layer was transformed into the $Co_3O_4$ phase. On the other hand, a sample without cobalt showed the usual $Cr_2O_3$ and $FeCr_2O_4$ phases.

## 3. Conclusions

The electrodeposition remains a very important topic for technology development. Through changes in operating parameters, one can obtain metallic or oxide films with different characteristics. The electrodeposited $Co_3O_4$, have an excellent supercapacitive behavior with specific capacitive value around 2700 $Fg^{-1}$. The $MnO_2$ synthesized by electrodeposition method also have very good values of supercapacitance varying between 240 and 521 $Fg^{-1}$. In solar cells, the electrodeposition is a very promising method for electrodes fabrication. This is because the electrodeposition is a method simple, practical and inexpensive to produce both p-type as n-type. Moreover, with the advancement of Solid Oxide Fuel Cells development, the electrodeposition is once again an important method to be considered. In this case the electrodeposition is an excellent method for improved of electrical interconnects. Finally, there is also an environmental aspect of electrodeposition. This because the metals recycling of metals presents in spent batteries is made principally by electrodeposition method.

## Author details

Eric M. Garcia[1], Vanessa F.C. Lins[2] and Tulio Matencio[2]

1 Federal University of São João Del Rei- unit of Sete Lagoas, Minas Gerais, Sete Lagoas, Brazil

2 Federal University of Minas Gerais, Minas Gerais, Belo Horizonte, Brazil

## References

[1] Conway, B. E.Theory and Principles of Electrode Processes. Ronald, New York: 1965.

[2] Conway, B. E. Electrochemical Data. Elsevier, Amsterdam: 1952.

[3] Parsons, R. Handbook of Electrochemical Data. Butterworths, London: 1959.

[4] B J. O'M. Bockris and A. K. N. Reddy. Modern Electrochemistry. Vol. 2, Plenum, New York:1970

[5] M.B.J.G. Freitas, E.M. Garcia. Electrochemical recycling of cobalt from cathodes of spent lithium-ion batteries. Journal of Power Sources 2007; 171 953–959.

[6] Q.I.N. Chuan-li, L.U. Xing, Y.I.N. Ge-ping, B.A.I. Xu-duo, J.I.N. Zheng. Activated nitrogen-enriched carbon/carbon aerogel nanocomposites for supercapacitor applications. Transactions of Nonferrous Metals Society of China 2009;19 738-742.

[7] Q. Wang, Q. Cao, X. Wang, B. Jing, H. Kuang, L. Zhou. A high-capacity carbon prepared from renewable chicken feather biopolymer for supercapacitors. Journal of Power Sources 2013;225 101-107.

[8] Y. Zhang, J. Li, F. Kang, F. Gao, X. Wang. Fabrication and electrochemical characterization of two-dimensional ordered nanoporous manganese oxide for supercapacitor applications. International Journal of Hydrogen Energy 2012; 37 860-866.

[9] T. Yousefi, A. N. Golikand, M. H. Mashhadizadeh, M. Aghazadeh, Template-free synthesis of $MnO_2$ nanowires with secondary flower like structure: Characterization and supercapacitor behavior studies. Current Applied Physics 2012:12 193-198.

[10] J.B. Wu,Y. Lin, X.H. Xia, J.Y. Xu, Q.Y. Shi, Pseudocapacitive properties of electrodeposited porous nanowall $Co_3O_4$ film Electrochimica 2011; 56 7163– 7170.

[11] G.X. Pan, X. Xia, F. Cao, P.S. Tang, H.F. Chen. Porous Co(OH)2/Ni composite nanoflake array for high performance supercapacitors. Electrochimica Acta 2012; 63 335–340.

[12] C.W Kung, H.W. Chen, C.Y. Lin, R. Vittal, K.C. Ho. Synthesis of $Co_3O_4$ nanosheets via electrodeposition followed by ozone treatment and their application to high-performance supercapacitors. Journal of Power Sources 2012: 214 91-99.

[13] W.J. Zhou, M.W. Xu, D.-D. Zhao, C.L. Xu, H.L. Li. Electrodeposition and characterization of ordered mesoporous cobalt hydroxide films on different substrates for supercapacitors. Microporous and Mesoporous Materials 2009; 117 55–60.

[14] Y. Asano, T. Komatsu, K. Murashiro, K. Hoshino. Capacitance studies of cobalt compound nanowires prepared via electrodeposition. Journal of Power Sources 2011; 196 5215–5222.

[15] Z. P. Feng, G. R. Li, J.H. Zhong, Z.L. Wang, Y.N. Ou, Y.X. Tong. $MnO_2$ multilayer nanosheet clusters evolved from monolayer nanosheets and their predominant electrochemical properties. Electrochemistry Communications 2009; 11 706–710.

[16] S. Chou, F. Cheng, J. Chen, Electrodeposition synthesis and electrochemical properties of nanostructured δ-MnO2 films. Journal of Power Sources 2006; 162 727–734.

[17] J. Nan, D. Han, M. Cui, M. Yang, L. Pan. Recycling spent zinc manganese dioxide batteries through synthesizing Zn–Mn ferrite magnetic materials. Journal of Hazardous Materials 2006; 133 257-261.

[18] Y. Gu, X. Su, Y. Du, C. Wang. Preparation of flower-like $Cu_2O$ nanoparticles by pulse electrodeposition and their electrocatalytic application Applied Surface Science 2010; 256 5862–5866.

[19] M. Fahoumea, O. Maghfoula, M. Aggoura, B. Hartitib, F. Chraı°bic, A. Ennaouic. Growth and characterization of ZnO thin films prepared by electrodeposition technique. Solar Energy Materials & Solar Cells 2006; 90 1437–1444.

[20] Y. Lai, Z. Chena, C. Hana, L. Jianga, F. Liua, J. Li, Y. Liu. Preparation and characterization of $Sb_2Se_3$ thin films by electrodeposition and annealing treatment Applied Surface Science 2012; 261 510– 514.

[21] W. Siripala. K.M.D.C. Jayathileka, J.K.D.S. Jayanetti. Low Cost Solar Cells with Electrodeposited Cuprous Oxide Journal of Bionanoscience 2009; 3 118–123.

[22] X. Han, K. Han, M. Tao, Characterization of Cl-doped n-type Cu2O prepared by electrodeposition Thin Solid Films 2010; 518 5363–5367.

[23] S. Thanikaikarasana, K. Sundarama, T. Mahalingama, S. Velumanib, J.K. Rheec. Electrodeposition and characterization of Fe doped CdSe thin films from aqueous solution. Materials Science and Engineering B 2010; 174 242–248.

[24] T.V. Nguyen, H.C. Lee, M. A. Khan, O.B. Yang. Electrodeposition of $TiO_2/SiO_2$ nanocomposite for dye-sensitized solar cell. Solar Energy 2007; 81 529–534.

[25] M.R. Ardigò, A. Perron, L. Combemale, O. Heintz, G. Caboche, S. Chevalier. Interface reactivity study between $La_{0.6}Sr_{0.4}Co_{0.2}Fe_{0.8}O_{(3-x)}$ (LSCF) cathode material and metallic interconnect for fuel cell Journal of Power Sources 2011; 196 2037–2045.

[26] P.Y. Chou, C.J. Ciou, Y.C. Lee, I.M. Hung. Effect of $La_{0.1}Sr_{0.9}Co_{0.5}Mn_{0.5}O_{(3-x)}$ protective coating layer on the performance of $La_{0.6}Sr_{0.4}Co_{0.8}Fe_{0.2}O_{(3-x)}$ solid oxide fuel cell cathode Journal of Power Sources 197 (2012) 12– 19

[27] Y. Zhen, S. P. Jiang, Characterization and performance of $(La,Ba)(Co,Fe)O_3$ cathode for solid oxide fuel cells with iron–chromium metallic interconnect. Journal of Power Sources 2008; 180 695–703.

[28] A. N. Hansson, S. Linderoth, M. Mogensen, M. A.J. Somers. Inter-diffusion between $Co_3O_4$ coatings and the oxide scale on Fe-22Cr. Journal of Alloys and Compounds 2007; 433 193–201.

[29] Z. Yang, G. Xia, P. Singh, J.W. Stevenson Electrical contacts between cathodes and metallic interconnects in solid oxide fuel cells. Journal of Power Sources 2006; 155 246–252.

[30] M. R. Bateni, P. Wei, X. Deng, A. Petric. Spinel coatings for UNS 430 stainless steel interconnects. Surface & Coatings Technology 2007; 201 4677–4684.

[31] J. Wu, Y. Jiang, C. Johnson, X. Liu, DC electrodeposition of Mn–Co alloys on stainless steels

[32] for SOFC interconnect application. Journal of Power Sources 2008; 177 376–385.

[33] X. Deng, P. Wei, M. R. Bateni, A Petric, Cobalt plating of high temperature stainless steel interconnects. Journal of Power Sources 2006; 160 1225–1229.

[34] E.M. Garcia, J.S. Santos, E.C. Pereira, M.B.J.G. Freitas, *Electrodeposition of cobalt from spent Li-ion battery cathodes by the electrochemistry quartz crystal microbalance technique.*. Journal of Power Sources 185 (2008) 549–553.

[35] M. B. J. G. Freitas, E. M. Garcia, V. G. Celante *Electrochemical and structural characterization of cobalt recycled from cathodes of spent Li-ion batteries* J Appl Electrochem (2009) 39:601–607

[36] E.M. Garcia, H. A. Tarôco, T. Matencio, R. Z. Domingues, J. A. F. dos Santos, R.V. Ferreira, E. Lorençon, D. Q. Lima, M.B.J.G. de Freitas. *Electrochemical recycling of cobalt from spent cathodes of lithium-ion batteries: its application as supercapacitor* J Appl Electrochem (2012) 42:361–366.

[37] E.M. Garcia, H. A. Tarôco, T. Matencio, R.Z. Domingues, J.A.F. dos Santos,M.B.J.G. de Freitas Electrochemical recycling of cobalt from spent cathodes of lithium–ion batteries: its application as coating on SOFC interconnects J Appl Electrochem (2011) 11:1373-1379.